Mathematics

https://www.aimspress.com/journal/Math

AIMS Mathematics, 11(8): 25295–25321.
DOI:10.3934/math.20261016
Received: 12 June 2026
Revised: 31 July 2026
Accepted: 04 August 2026
Published: 17 August 2026

Research article

Adaptive bipartite consensus for dynamic event-triggered multi-agent systems under DoS attacks

Xiaoli Ruan[1], Zhiwei Du[1], Huali Yang[1], Chen Wang[1] and Jianwen Feng[2,*]

[1] School of Computer Science and Aritificial Intelligence, Wuhan Textile University, Wuhan, China
[2] School of Mathematical Sciences, Shenzhen University, Shenzhen 518060, China

* **Correspondence:** Email: fengjw@szu.edu.cn.

Abstract: This paper studies the leader-following bipartite consensus issue for multi-agent systems (MASs) with event-triggered control strategy under denial-of-service (DoS) attacks. To prevent parameters from growing unboundedly during the adaptive process, a projection operator-based adaptive control algorithm combined with a distributed dynamic event-triggered (DET) control strategy is introduced. This control strategy can also reduce unnecessary communication burden. Unlike most existing control algorithms for structurally balanced graphs, a partition algorithm is used to achieve bipartite consensus for the structurally unbalanced case. Besides, by utilizing LMI technology and the Lyapunov function method, several criteria are established to guarantee the stability of error systems under DoS attacks. Moreover, a proof by contradiction is employed to rule out Zeno behavior. Finally, the effectiveness and superiority of the proposed approach are verified by a simulation example.

Keywords: event-triggered control; multi-agent systems; bipartite consensus; Zeno behavior
Mathematics Subject Classification: 93C27

1. Introduction

Over the past two decades, the consensus problem of multi-agent systems (MASs) has attracted considerable attention from both academia and industry due to its superior performance and wide application scenarios, such as multi-robot collaboration, spacecraft coordination, and vehicular networks [1–3]. Based on the high robustness and flexible scalability of MASs, remarkable achievements have been made in the study of cooperative control problems for such systems [4–6]. It is worth noting that the aforementioned achievements only consider cooperative relationships among agents, meaning that all weights in the communication topologies are positive. However, in practical engineering, there exist not only cooperative but also competitive relationships between agents, such as the bidirectional formation flight of autonomous aerial vehicles and the mutual confrontation between robots in soccer competitions [7]. Therefore, investigating the coexistence mechanism of cooperation and competition has more practical application value.

The bipartite consensus issue for cooperative-competitive MASs has been extensively studied [8–10]. In existing bipartite consensus control research, common control methods include event-triggered control [11], impulsive control [12], feedback control [13], intermittent control [14], etc. Among them, event-triggered control has gained popularity among scholars due to its ability to save energy resources and effectively avoid continuous communication [15]. For example, in reference [16], a distributed event-triggered strategy was introduced to solve the leader-following bipartite consensus issue. [17] introduced a novel composite event-triggered control scheme for a fully distributed bipartite compensator. This scheme achieves resource optimization. To further optimize the event-triggered control strategy [18, 19], a dynamic event-triggered (DET) distributed model-predictive control algorithm was proposed to dynamically adjust the trigger threshold, thereby reducing computational and communication burdens. However, these studies assume that communication channels are secure, whereas the consensus control of MASs heavily relies on information exchange over communication networks, rendering such networks vulnerable to cyber attacks that can cause system instability.

Various cyberattacks threaten MASs, including Byzantine attacks [20], deception attacks [21], and denial-of-service (DoS) attacks [22]. Among the myriad malicious attacks, the DoS attack is the most common and dangerous form of network attack, which aims to disrupt system stability by preventing information transmission between agents. For the bipartite consensus problem in MASs, a large number of studies have considered the impact of DoS attacks and proposed corresponding countermeasures [23]. For example, in reference [24], a bipartite containment control protocol featuring a resilient event-triggered scheme was presented, which enabled MASs to withstand DoS attacks while improving resource efficiency and fulfilling the control goal. In [25], a fully distributed bipartite consensus problem was studied for MASs subjected to DoS attacks. Reference [26] studied a bipartite containment control algorithm for MASs with external disturbances, where an attack compensator is introduced to mitigate the adverse impacts of DoS attacks. Although [24–26] achieved significant results in combating DoS attacks, the above results mainly consider structurally balanced topology. How to achieve bipartite consensus control of MASs under network attacks in unbalanced communication topology is worth further study. Recently, a classification optimization algorithm based on unbalanced communication topology graph was proposed in the references [27, 28] to achieve bipartite consensus, which makes the research more general, but resource saving was not considered.

It is observed that the above control strategies all adopt the same constant gain. Such a uniform gain often results in redundant inter-agent signal transmission. Therefore, a distributed adaptive control scheme was proposed to dynamically adjust the coupling gain [29, 30]. However, in the presence of noise and interference, the coupling gain may still gradually increase when the system has achieved consensus. To solve this problem, reference [31] proposed a distributed control method based entirely on projection operators, which restricts the adaptive gain to operate within a specific region without the need to know the exact structure of the constraint set in advance. The scarcity of research on bipartite consensus for competitive MASs under DoS attacks, particularly those with unbalanced communication topology and using projection operator-based adaptive DET control, provides the primary impetus for this article.

Compared with the existing studies [23, 32], the proposed framework does not simply place the partition algorithm, projection operator, and DET mechanism in parallel. The partition algorithm first extracts a useful topology and determines the antagonistic camps, thereby providing a suitable transformed Laplacian matrix for the subsequent control design. Based on this topology, the projection-based adaptive law and the DET condition are coupled through the same sampled disagreement variables, so that gain regulation and transmission decisions enter a unified stability analysis. Furthermore, the controller, adaptive law, and dynamic triggering variable are coordinated over the safe and effective DoS intervals, including the post-attack recovery delay. This coupling distinguishes the proposed method from existing results considering these issues separately.

Motivated by the above observations, this paper investigates the bipartite consensus problem for MASs with a structurally unbalanced graph under DoS attacks using DET schemes. Specifically, a projection operator-based adaptive protocol integrated with DET control is developed to ensure the closed-loop system stability. The main contributions are threefold:

1) Different from [27,28], this paper proposes a DET scheme incorporating adaptive coupling gains for MASs with DoS attacks, in which the proposed projection operator-based adaptive updating gains are always maintained within a constrained feasible set to prevent unbounded parameter growth during adaptation.

2) In the previous works, most bipartite consensus control of MASs is based on the structurally balanced graph [24–26]. We used a partition algorithm and projection operator-based adaptive DET control scheme to achieve the bipartite consensus based on the structurally unbalanced communication topology, which is more general and challenging.

3) Unlike the work in [23,33], which deals with DoS attacks without DoS-induced delay, this paper incorporates DoS-induced delays to reflect realistic scenarios where communication may fail to resume promptly after an attack.

Notations: Define $\mathbb{R}$ and $\mathbb{R}^+$ as the sets of real and positive real numbers, respectively. $\mathbb{R}^{n\times m}$ denotes the space of $n \times m$ real matrices. $\|\cdot\|$ is the Euclidean vector norm, $sgn(\cdot)$ the sign function, and $\otimes$ the Kronecker product.

2. Preliminaries

2.1. Graph theory

Let $G = (\mathcal{V}, E, \mathcal{A})$ be a signed graph, which consists of a set of nodes $\mathcal{V} = \{v_1, \ldots, v_N\}$ and a set of edges $E \subseteq \mathcal{V} \times \mathcal{V}$. A signed adjacency matrix is $\mathcal{A} = [a_{ij}]_{N\times N} \in \mathbb{R}^{N\times N}$. If $a_{ij} > 0$, the relationship between v_j and v_i is cooperative; if $a_{ij} < 0$, it is competitive. The Laplacian matrix $L = [l_{ij}]_{N\times N} \in \mathbb{R}^{N\times N}$ is defined as

$$l_{ij} = \begin{cases} -a_{ij}, & i \neq j, \\ \sum\limits_{\substack{j=1 \\ j\neq i}}^{N} |a_{ij}|, & i = j. \end{cases}$$

The leader v_0 is taken into consideration in the network, then let $\overline{G} = G \cup \{v_0\} = (\overline{\mathcal{V}}, \overline{E}, \mathcal{A})$ be another signed digraph, where $\overline{\mathcal{V}} = \mathcal{V} \cup \{v_0\}$ and $\overline{E} \subseteq \overline{\mathcal{V}} \times \overline{\mathcal{V}}$. Define the matrix $\tilde{L} = L + L_0$, where $L_0 = diag\{l_{10}, l_{20}, \cdots, l_{N0}\}$ denotes the connection from the leader to the followers. The signed digraph $\overline{G}$ considered in this paper is structurally unbalanced.

Definition 2.1. *In the signed undirected graph G, the shortest path along which node $v_{i,1}$ receives messages from node $v_{i,j}$ is given by $L_i = \min\{(v_{i,1}, v_{i,2}),\ (v_{i,2}, v_{i,3}),\ \ldots,\ (v_{i,j-1}, v_{i,j})\}$. The path $L_i > 0$, if the edge signs satisfy $a_{i_2,i_1} \cdot a_{i_3,i_2} \cdots a_{i_j,i_{j-1}} > 0$; otherwise, $L_i < 0$. (Here, v_{i_{k+1},i_k} represents the sign or weight attached to the undirected edge $(v_{i_k}, v_{i_{k+1}})$, and because the graph is undirected, we have $a_{i_{k+1},i_k} = a_{i_k,i_{k+1}}$.)*

Assumption 2.1. *The signed undirected graph $\overline{G}$ is connected.*

2.2. A partition algorithm

To address the structural unbalance in the original undirected graph, a partition algorithm based on node state signs is employed to reconstruct the topology. According to Definition 1, the proposed partition algorithm divides nodes into two sets $\bar{q}_1$ and $\bar{q}_2$, which satisfy $\bar{q}_1 \cap \bar{q}_2 = \emptyset$, $\bar{q}_1 \cup \bar{q}_2 = \mathcal{V}$. Moreover, $i, j \in \bar{q}_e$ $(e \in \{1, 2\})$ if and only if $a_{ij} \geq 0$, and $i \in \bar{q}_e, j \in \bar{q}_{3-e}$ $(e \in \{1, 2\})$ if and only if $a_{ij} \leq 0$. S is defined as $S = \mathrm{diag}\{l_1, l_2, \ldots, l_N\}$, where $l_i = 1$ if $i \in \bar{q}_1$ and $l_i = -1$ if $i \in \bar{q}_2$. The detailed process is presented in Algorithm 1. The Laplacian matrix corresponding to the modified topology is denoted as $\overline{L}$, which satisfies a specific decomposition relationship with the original matrix. Consequently, due to the structural transformation executed by Algorithm 1, the elements of $\tilde{L}$ and the associated parameters l_{ij} are updated accordingly. This algorithm aims to eliminate structural conflicts, thereby ensuring that the system can effectively converge to bipartite consensus.

Based on the above Algorithm 1, we can obtain the following conditions: $S\mathcal{A}S = \tilde{\mathcal{A}}$ and $S\bar{L}S = \hat{L}$, where $\tilde{\mathcal{A}} = (|a_{ij}|)_{N\times N}$ and $\hat{L}$ denote the adjacency matrix and Laplacian matrices of the corresponding unsigned graph $\tilde{\mathcal{G}}$, respectively. Then, denote the smallest and largest eigenvalues of $\hat{L}$ as $\lambda_{\min}(\hat{L})$ and $\lambda_{\max}(\hat{L})$, respectively.

Remark 2.1. *Under Assumption 2.1, the leader-augmented signed undirected graph is finite and connected. Therefore, every follower has a finite distance from the leader, and each node in M_h has at least one candidate parent in M_{h-1}. Since every follower is assigned once, Algorithm 1 terminates after at most N layers. For each selected parent edge (v_j, v_i), the assignment $l_i = l_j\,\mathrm{sgn}(a_{ij})$ yields $l_i a_{ij} l_j = |a_{ij}| > 0$. By induction over the distance layers, all retained edges of the modified topology satisfy the prescribed intra-camp and inter-camp sign relationships. This establishes the correctness of the partition and leads to $S\mathcal{A}S = \tilde{\mathcal{A}}$ and $S\bar{L}S = \hat{L}$ for the modified topology. The maximum-weight rule together with the minimum-index tie-breaking rule produces a deterministic partition for a fixed leader, node labeling, and edge weights. Nevertheless, the result is not claimed to be globally optimal, and different leaders or tie-breaking rules may produce different modified topologies. The computational complexity is $O(N+|\mathcal{E}|)$ using adjacency lists and $O(N^2)$ using an adjacency matrix. The algorithm is applicable to finite, connected, static signed undirected graphs; disconnected, directed, or time-varying graphs require further extensions.*

2.3. Mathematical model

Consider an MAS consisting of N followers, and the dynamics can be expressed as

$$\dot{x}_i(t) = Ax_i(t) + Bu_i(t), \tag{2.1}$$

Algorithm 1 Node Partition Algorithm for Signed Undirected Graphs

Require: Signed undirected graph $G = (\mathcal{V}, E, \mathcal{A})$, leader node v_0.
Ensure: For sets $\bar{q}_1$ and $\bar{q}_2$, $\bar{q}_1 \cup \bar{q}_2 = \mathcal{V}$.

Initialization:
Calculate the shortest path length L_i for all nodes $v_i \in \mathcal{V}$ relative to v_0.
Construct sets $M_0 = \{v_0\}$ and $M_h = \{v_i \mid L_i = h\}$ for $h = 1, \ldots, \chi$.
Set $\bar{q}_1 \leftarrow \{v_0\}$, $\bar{q}_2 \leftarrow \emptyset$.
Assign sign value $S(v_0) \leftarrow 1$ (Positive).
Main Loop:
for $h = 1$ to χ **do**
    for each node $v_i \in M_h$ **do**
        // Step 1: Identify candidate parent nodes in M_{h-1}
        Let $\mathcal{P}_i = \{v_k \in M_{h-1} \mid \{v_k, v_i\} \in E\}$.
        // Step 2: Select the unique parent v_j based on max weight
        Find v_j that satisfies the criterion:
        $j = \min\{k \mid |a_{i,k}| = \max_{v_l \in \mathcal{P}_i} |a_{i,l}|\}$.
        // Step 3: Determine path sign and partition
        Calculate sign of unique path: $S(v_i) = S(v_j) \times \mathrm{sgn}(a_{i,j})$.
        if $S(v_i) > 0$ **then**
            $\bar{q}_1 \leftarrow \bar{q}_1 \cup \{v_i\}$
        else
            $\bar{q}_2 \leftarrow \bar{q}_2 \cup \{v_i\}$
        end if
    end for
end for
return $\bar{q}_1, \bar{q}_2$

where $x_i(t) \in \mathbb{R}^n$ and $u_i(t) \in \mathbb{R}^m$ represent the state vector and the control input of i-th follower, A, B are constant matrices. The leader can be denoted as

$$\dot{x}_0(t) = Ax_0(t),$$

where $x_0(t) \in \mathbb{R}^n$.

Definition 2.2. *For any initial condition $x_i(0), i = 1, \ldots, N$, the MAS given in (2.1) is said to achieve bipartite consensus if*

$$\lim_{t\to\infty} \|x_i(t) - s_i x_0(t)\| = 0, \quad i \in N.$$

Assumption 2.2. *The matrix pair (A, B) in (2.1) is stabilizable.*

2.4. DoS attacks model

This study focuses on MASs subject to DoS attacks, where the attacks are imposed on the controller of each individual agent rather than on communication edges. Specifically, for agent i, the control input may be maliciously blocked during certain time intervals, which leads to temporary controller failure. Let $\{T_k\}$ denote the sequence of attack starting instants acting on the controller of agent i, and let τ_k be the finite duration of the k-th attack. Then, the corresponding attack interval is defined as $I_k = [T_k, T_k + \tau_k)$. During this interval, the controller of agent i is disabled, and the control input is assumed to satisfy $u_i(t) = 0$. After each attack interval, the adversary enters an attack-free period, denoted by $[T_k + \tau_k, T_{k+1})$, during which the controller of agent i recovers and normal control updates can be applied. The alternating occurrence of attack-active and attack-free periods reflects a practical intermittent attack pattern in real networked control systems.

In practice, the end of a DoS attack does not necessarily imply the immediate recovery of the controller. Due to signal retransmission, controller restarting, or information resynchronization, a DoS-induced recovery delay may occur after each attack interval. Let χ_k denote the recovery delay following the k-th DoS attack, where $0 \leq \chi_k \leq \chi$ and $\chi > 0$ is a known upper bound. Then, the effective DoS interval can be described as $I_k^* = [T_k, T_k + \tau_k + \chi_k)$. During I_k^*, the controller of agent i is regarded as unavailable, and valid control updates can only be resumed after $T_k + \tau_k + \chi_k$. Thus, the DoS-induced delay enlarges the actual unavailable period of the controller and provides a more realistic description of intermittent attack effects in MASs.

For agent i, the set of all time instants affected by DoS attacks over the interval $[t_a, t_b)$ is given by

$$\Psi_{att}(t_a, t_b) = \bigcup_{k \in \mathbb{N}^+} I_k^* \cap [t_a, t_b).$$

Similarly, the corresponding attack-free time set over $[t_a, t_b)$ is defined as

$$\Phi_{safe}(t_a, t_b) = [t_a, t_b) \setminus \Psi_{att}(t_a, t_b).$$

Assumption 2.3. ***(DoS duration).*** *For any time interval $[t_0, t)$, the total duration of DoS attacks is assumed to be bounded. Specifically, there exist constants $N_1 \geq 0$ and $\Omega_1 > 1$ such that*

$$\Psi(t_0, t) \leq N_1 + \frac{t - t_0}{\Omega_1},$$

where $\Psi(t_0, t)$ denotes the total length of DoS attack intervals over $[t_0, t)$.

Assumption 2.4. ***(DoS frequency).*** *For any time interval $[t_0, t)$, the occurrence frequency of DoS attacks is constrained by an average dwell-time-type condition. That is, there exist constants $N_2 \geq 0$ and $\Omega_2 > 0$ satisfying*

$$\wp(t_0, t) \leq N_2 + \frac{t - t_0}{\Omega_2},$$

where $\wp(t_0, t)$ represents the number of DoS attacks occurring during $[t_0, t)$.

Remark 2.2. *It should be noted that a recovery delay may arise after each DoS attack ends, since the communication among agents may not be restored immediately. To characterize this effect, each DoS interval is upper bounded by a positive constant χ. Let $\Psi^*_{\text{att}}(t_0, t)$ be the union of the valid DoS attack intervals on $[t_0, t)$. Then, let $\Psi^*_{\text{att}}(t_0, t) \leq \Psi(t_0, t) + \wp(t_0, t)\chi$. Similarly, $\Psi^*_{\text{safe}}(t_0, t)$ represent the union of the valid safe intervals over $[t_0, t)$. Hence, $\Psi^*_{\text{safe}}(t_0, t) = t - t_0 - \Psi^*_{\text{att}}(t_0, t)$.*

Remark 2.3. *Assumptions 2.3 and 2.4 follow the standard duration-frequency characterization of DoS attacks [34]. From a switched-system perspective, the DoS-affected error system alternates between a controlled safe mode and a controller-unavailable attack mode. This interpretation differs from that of switching-topology MASs: In the latter, the adjacency and Laplacian matrices vary with time, whereas in this work the signed graph and its Laplacian matrix remain fixed, and only the availability of the controller is switched by the DoS signal. Assumption 2.3 bounds the cumulative residence time in the attack mode, while Assumption 2.4 is an average dwell-time-type constraint that limits the occurrence frequency of DoS intervals. Both constraints are required because frequent short attacks may introduce a significant cumulative recovery delay even when their original duration is small. Since* $0 \leq \chi_k \leq \chi$, *the effective DoS duration satisfies* $|\Psi^*_{\text{att}}(t_0,t)| \leq |\Psi_{\text{att}}(t_0,t)| + \chi\wp(t_0,t) \leq N_1 + N_2\chi + \left(\frac{1}{\Omega_1} + \frac{\chi}{\Omega_2}\right)(t-t_0)$. *This estimate is used in Theorem 3.1 to ensure that the Lyapunov decay accumulated during the safe intervals dominates the possible growth during the effective DoS intervals.*

We aim to introduce an adaptive control framework for MASs under DoS attacks, which forces all error system signals to approach zero. The next section presents the main results.

3. Main results

This section mainly develops an adaptive DET control strategy to reduce the communication burden and achieve bipartite consensus for MAS (2.1) that suffers from DoS attacks.

3.1. Adaptive DET control strategy

The adaptive DET control scheme in this paper is developed in two stages: first, a projection-operator-based nominal adaptive control, followed by the design of a DET control. Denote the triggering instant as t^i_k ($k \in Z^+$), where the triggering times $0 = t^i_1 < \cdots < t^i_k < \cdots$ are decided by the DET condition (3.2). For $t \in [t^i_k, t^i_{k+1})$, let $\hat{x}_i(t) = x_i(t^i_k)$. Similarly, $\hat{x}_j(t)$ and $\hat{x}_0(t)$ denote the most recently received states of neighbor j and the leader, respectively. Then, an adaptive DET consensus control strategy is developed as

$$
\begin{aligned}
u_i(t) &= \hat{c}_i(t)K(\sum_{j=1}^{N}|a_{ij}|(\hat{x}_i(t) - sgn(a_{ij})\hat{x}_j(t)) + |l_{i0}|(\hat{x}_i - s_i\hat{x}_0)),\\
\dot{\hat{c}}_i(t) &= \begin{cases} cProj_i(\hat{c}_i, M_i), & \text{if } t \in \Phi_{safe}(0,t),\\ 0, & \text{if } t \in \Psi_{att}(0,t),\end{cases}
\end{aligned}
$$

where $K = -B^\top P$ is the feedback gain matrix, and $c > 0$. For convenience, we will replace $\hat{c}_i(t)$ with $\hat{c}_i$ next.

Let $\theta = \{\hat{c}_i \in \mathbb{R} : (\underline{c} \leq \hat{c}_i \leq \bar{c}); \quad i = 1,\ldots,n\}$, where $\underline{c}$ and $\bar{c}$ are the minimum and maximum limits of $\hat{c}_i$ in the set θ. Furthermore, for a sufficiently small constant $\varepsilon > 0$, define the compact convex set $\theta_\varepsilon = \left\{\hat{c}_i \in \mathbb{R} : \underline{c} + \varepsilon \leq \hat{c}_i \leq \bar{c} - \varepsilon,\ i = 1,\ldots,N\right\}$, where $\theta_\varepsilon \subset \theta$. The projection operator

$\text{Proj}_i(d_i, M_i) : \mathbb{R} \times \mathbb{R} \to \mathbb{R}$ is defined component wise as

$$Proj_i(\hat{c}_i, M_i) = \begin{cases} (\frac{\bar{c}-\hat{c}_i}{\varepsilon})M_i, & \text{if } \hat{c}_i > \bar{c} - \varepsilon, \\ (\frac{\hat{c}_i-\underline{c}}{\varepsilon})M_i, & \text{if } \hat{c}_i < \underline{c} + \varepsilon, \\ M_i, & \text{otherwise,} \end{cases} \tag{3.1}$$

where $M_i = e^{\alpha t}\hat{q}_i^\top(t)\Gamma\hat{q}_i(t)$, $\hat{q}_i(t) = \sum_{j=1}^{N} |a_{ij}|(\hat{x}_i(t) - sgn(a_{ij})\hat{x}_j(t)) + |l_{i0}|(\hat{x}_i(t) - s_i\hat{x}_0(t))$. Due to M_i is projected onto the constrained set θ, the projection operator

$$(\hat{c}_i - \beta)(Proj_i(\hat{c}_i, M_i) - M_i) \le 0$$

holds for a given $\beta \in \theta$, where $\beta \in \mathbb{R}$.

Remark 3.1. *In [32], to overcome difficulties caused by disturbances and other uncertainties, the corresponding control method adjusts the coupling gain until it reaches a prescribed upper bound, after which the adaptation process is terminated. However, the determination of this bound still depends on global information of the Laplacian matrix. In contrast, the proposed control method in (3.1) employs the projection operator to constrain the adaptive coupling gain $\hat{c}_i$ within a prescribed compact set θ. This mechanism prevents the adaptive gain from unbounded growth while preserving the distributed nature of the controller. Moreover, since the exact upper bound required by the graph topology is not explicitly needed in the controller design, $\bar{c}$ can be selected sufficiently large, thereby relaxing the dependence on global graph information.*

Next, denote $\delta_i(t) = x_i(t) - s_i x_0(t)$ as the bipartite consensus error. Let $\hat{\delta}_i(t) = \hat{x}_i(t) - s_i\hat{x}_0(t)$ and $\tilde{\delta}_i(t) = \delta_i(t) - \hat{\delta}_i(t)$, which stand for estimation error and error difference, respectively.

Let $\tilde{x}_i(t) = x_i(t) - \hat{x}_i(t)$, then t_{k+1}^i is obtained from the DET condition as follows:

$$t_{k+1}^i = \inf\{t > t_k^i : t \in \Phi_{safe}, \theta_i[\hat{c}_i(t)\tilde{q}_i^\top(t)\Gamma\tilde{q}_i(t) - \frac{\kappa\beta}{\ell}\hat{q}_i^\top(t)\Gamma\hat{q}_i(t)] > \eta_i(t)\}, \tag{3.2}$$

where constant $\theta_i > 0$, $\kappa = -\frac{(\varepsilon_1-1)(1-\varepsilon_2)}{\lambda_{\max}(\hat{L})} > 0$, $\ell = \frac{\kappa}{\varepsilon_2} + \frac{1}{\varepsilon_1\lambda_{\max}(\hat{L})} > 0$, and $\tilde{q}_i(t) = \sum_{j=1}^{N} |a_{ij}|(\tilde{x}_i(t) - sgn(a_{ij})\tilde{x}_j(t)) + |l_{i0}|(\tilde{x}_i(t) - s_i\tilde{x}_0(t))$. The parameters Γ, ε_1, and ε_2 will be specified later.

Besides, $\eta_i(t)$ satisfies:

$$\dot{\eta}_i(t) = \begin{cases} -\rho_i\eta_i(t) - \frac{\xi_i}{\theta_i}\eta_i(t), & \text{if } t \in \Phi_{safe}(0,t), \\ 0, & \text{if } t \in \Psi_{att}(0,t), \end{cases} \tag{3.3}$$

where $\eta_i(0) > 0$, $\rho_i > 0$, and $\xi_i > 0$. It follows from (3.3) that

$$\eta_i(t) = \eta_i(0)\exp\left[-\left(\rho_i + \frac{\xi_i}{\theta_i}\right)|\Phi_{\text{safe}}(0,t)|\right] > 0.$$

Therefore, $\sum_{i=1}^{N} \eta_i(t)$ is nonnegative for all $t \ge 0$.

Under Assumption 2.2, for given matrix $Q > 0$, the following algebraic Riccati equation

$$A^T P + PA - \underline{c}\lambda_{\min}(\hat{L})\Gamma + Q = 0$$

has a unique solution $P > 0$. Thus, let $K = -B^\top P$, $\Gamma = PBB^\top P$.

Theorem 3.1. *Under Assumptions 2.3 and 2.4, bipartite consensus of MASs using the DET control protocol in the presence of DoS attacks is guaranteed if the following condition holds:*

$$\frac{1}{\Omega_1} + \frac{\chi}{\Omega_2} \leq \frac{\alpha}{\alpha + \hat{\alpha}}, \tag{3.4}$$

where two positive constants $\alpha = \min\{\frac{\lambda_{\min}(Q)}{\lambda_{\max}(P)}, \rho_i + \frac{\xi_i - \ell}{\theta_i}\}$, $\hat{\alpha} = \frac{\lambda_{\max}(A^T P + PA)}{\lambda_{\min}(P)} > 0$, *and* ρ_i, β, *and* θ_i *will be specified later.*

Remark 3.2. *The main difficulty introduced by the recovery delay is that the controller cannot resume immediately after an attack, and the consensus error may continue to evolve under the uncontrolled dynamics during the recovery phase. Since the recovery delay occurs after every attack, its cumulative effect depends on both the delay bound and the attack frequency, leading to the additional term* χ/Ω_2 *in the stability condition. Here,* α *represents the error decay rate during safe intervals,* $\hat{\alpha}$ *characterizes the possible error growth during effective DoS intervals, and* $1/\Omega_1$ *and* $1/\Omega_2$ *reflect the DoS-duration ratio and attack frequency, respectively. The parameters should satisfy* $\frac{1}{\Omega_1} + \frac{\chi}{\Omega_2} < \frac{\alpha}{\alpha+\hat{\alpha}}$, *and the maximum admissible recovery delay is* $\chi_{\max} = \Omega_2\left(\frac{\alpha}{\alpha+\hat{\alpha}} - \frac{1}{\Omega_1}\right)$. *Thus, increasing* χ *linearly decreases the guaranteed convergence margin in (3.18). Since this condition is derived using worst-case bounds, it is sufficient and may be conservative. For the projection interval* $[\underline{c}, \bar{c}]$, $\underline{c}$ *should provide sufficient coupling strength, whereas* $\bar{c}$ *should avoid premature gain saturation while satisfying actuator limitations, with the initial adaptive gain selected inside this interval.*

Proof. We choose the Lyapunov function as

$$V_1(t) = \delta^\top(t)(I_N \otimes P)\delta(t),$$

$$V_2(t) = \sum_{i=1}^{N} \eta_i(t),$$

$$V_3(t) = \frac{\kappa}{2c}\sum_{i=1}^{N}(\hat{c}_i - \beta)(\hat{c}_i - \beta),$$

and

$$U(t) = V_1(t) + V_2(t),$$

$$W(t) = e^{\alpha t}U(t) + V_3(t).$$

The exponential term $e^{\alpha t}$ acts as an integrating factor. It is introduced to incorporate the desired decay rate α into the Lyapunov analysis and to compare the decay accumulated during the safe intervals with the possible growth during the DoS intervals. For notational convenience, set $\delta(t) = [\delta_1^T(t), \delta_2^T(t), \ldots, \delta_N^T(t)]^T$, $\hat{\delta}(t) = [\hat{\delta}_1^T(t), \hat{\delta}_2^T(t), \ldots, \hat{\delta}_N^T(t)]^T$, $\tilde{\delta}(t) = [\tilde{\delta}_1^T(t), \tilde{\delta}_2^T(t), \ldots, \tilde{\delta}_N^T(t)]^T$, and $\hat{q}(t) = [\hat{q}_1^T(t), \ldots, \hat{q}_N^T(t)]^T$.

Then, the subsequent analysis is carried out separately for two cases, namely the attack-active intervals and the intervals without attacks.

Case 1: When the agent is free of attacks, differentiating $\delta_i(t) = x_i(t) - s_i x_0(t)$ gives

$$\dot{\delta}_i(t) = A\delta_i(t) + Bu_i(t).$$

According to Algorithm 1 and the definition of the pinned signed Laplacian matrix $\bar{L}$, the sampled disagreement vector satisfies $\hat{q}(t) = (\bar{L}\otimes I_n)\hat{\delta}(t)$. Define $\hat{c} = \mathrm{diag}\{\hat{c}_1(t), \ldots, \hat{c}_N(t)\}$. By stacking the error dynamics and substituting $u(t) = (\hat{c}(t) \otimes K)\hat{q}(t)$ and $K = -B^\top P$, we obtain

$$\dot{\delta}(t) = (I_N \otimes A)\delta(t) - (\hat{c}(t) \otimes BB^\top P)\hat{q}(t). \tag{3.5}$$

Then, substituting (3.5) into the $\dot{V}_1(t)$, one obtains

$$\begin{aligned}
\dot{V}_1(t) &= \delta^T(t)(I_N \otimes (A^T P + PA))\delta(t) - 2\delta^T(t)(\hat{c} \otimes \Gamma)\hat{q}(t)\\
&= \delta^T(t)(I_N \otimes (A^T P + PA))\delta(t) - 2\delta^T(t)(\hat{c}\bar{L} \otimes \Gamma)\hat{\delta}(t)\\
&= \delta^T(t)(I_N \otimes (A^T P + PA))\delta(t) - 2\delta^T(t)(\hat{c}\bar{L} \otimes \Gamma)\delta(t) + 2\delta^T(t)(\hat{c}\bar{L}(t) \otimes \Gamma)\tilde{\delta}(t).
\end{aligned} \tag{3.6}$$

Regarding the final item of (3.6),

$$\begin{aligned}
2\delta^T(t)(\hat{c}\bar{L} \otimes \Gamma)\tilde{\delta}(t) &= 2\delta_s^T(t)(\hat{c}\hat{L} \otimes \Gamma)\tilde{\delta}_s(t)\\
&\leq \varepsilon_1\delta_s^\top(t)(\hat{c}\hat{L} \otimes \Gamma)\delta_s(t) + \frac{1}{\varepsilon_1}\tilde{\delta}_s^\top(t)(\hat{c}\hat{L} \otimes \Gamma)\tilde{\delta}_s(t),
\end{aligned} \tag{3.7}$$

where $S\bar{L}S = \hat{L}$, $0 < \varepsilon_1 < 1$, and $\delta_s(t) = (S \otimes I_N)\delta(t)$, $\tilde{\delta}_s(t) = (S \otimes I_N)\tilde{\delta}(t)$.

Because of $\delta_i(t) = \hat{\delta}_i(t) + \tilde{\delta}_i(t)$, from (3.7), we have

$$\begin{aligned}
\dot{V}_1(t) \leq\ & \delta^T(t)(I_N \otimes (A^T P + PA))\delta(t) - \delta_s^T(t)(\hat{c}\hat{L} \otimes \Gamma)\delta_s(t)\\
&- \delta_s^T(t)(\hat{c}\hat{L} \otimes \Gamma)\delta_s(t) + \varepsilon_1\delta_s^T(t)(\hat{c}\hat{L} \otimes \Gamma)\delta_s(t) + \frac{1}{\varepsilon_1}\tilde{\delta}_s^T(\hat{c}\hat{L} \otimes \Gamma)\tilde{\delta}_s(t)\\
\leq\ & \delta^T(t)(I_N \otimes (A^T P + PA))\delta(t) - \underline{c}\lambda_{\min}(\hat{L})\delta_s^T(t)\Gamma\delta_s(t)\\
&- \delta_s^T(t)(\hat{c}\hat{L} \otimes \Gamma)\delta_s(t) + \varepsilon_1\delta_s^T(t)(\hat{c}\hat{L} \otimes \Gamma)\delta_s(t) + \frac{1}{\varepsilon_1}\tilde{\delta}_s^T(\hat{c}\hat{L} \otimes \Gamma)\tilde{\delta}_s(t)\\
\leq\ & \delta^T(t)(I_N \otimes (A^T P + PA) - \underline{c}\lambda_{\min}(\hat{L}) \otimes \Gamma)\delta(t)\\
&+ (\varepsilon_1 - 1)\delta_s^T(t)(\hat{c}\hat{L} \otimes \Gamma)\delta_s(t) + \frac{1}{\varepsilon_1}\tilde{\delta}_s^T(\hat{c}\hat{L} \otimes \Gamma)\tilde{\delta}_s(t),
\end{aligned} \tag{3.8}$$

where $q(t) = [q_1^T(t), \ldots, q_N^T(t)]^T$, $q_s(t) = (\hat{L} \otimes I_N)\delta_s(t)$, and $\tilde{q}_s(t) = (\hat{L} \otimes I_N)\tilde{\delta}_s(t)$. Then,

$$\begin{aligned}
&(\varepsilon_1 - 1)\delta_s^T(t)(\hat{c}\hat{L} \otimes \Gamma)\delta_s(t)\\
\leq\ & \frac{\varepsilon_1 - 1}{\lambda_{\max}(\hat{L})}q_s^T(t)(\hat{c} \otimes \Gamma)q_s(t)\\
\leq\ & \frac{\varepsilon_1 - 1}{\lambda_{\max}(\hat{L})}\sum_{i=1}^{N}\hat{c}_i q_i^T\Gamma q_i(t)
\end{aligned}$$

$$\leq \frac{(\varepsilon_1-1)(1-\varepsilon_2)}{\lambda_{\max}(\hat{L})}\sum_{i=1}^{N}\hat{c}_i\hat{q}_i^T(t)\Gamma\hat{q}_i(t)+\frac{(\varepsilon_1-1)(1-\frac{1}{\varepsilon_2})}{\lambda_{\max}(\hat{L})}\sum_{i=1}^{N}\hat{c}_i\tilde{q}_i^T(t)\Gamma\tilde{q}_i(t), \tag{3.9}$$

where $0<\varepsilon_2<1$. Substituting (3.9) into (3.8) yields

$$\begin{aligned}
\dot{V}_1(t) \leq\, & \delta_s^T(t)(I_N\otimes(A^TP+PA)-\underline{c}\lambda_{\min}(\hat{L})\otimes\Gamma)\delta_s(t)\\
&+\frac{(\varepsilon_1-1)(1-\varepsilon_2)}{\lambda_{\max}(\hat{L})}\sum_{i=1}^{N}\hat{c}_i\hat{q}_i^\top(t)\Gamma\hat{q}_i(t)+\frac{(\varepsilon_1-1)(1-\frac{1}{\varepsilon_2})}{\lambda_{\max}(\hat{L})}\sum_{i=1}^{N}\hat{c}_i\tilde{q}_i^T(t)\Gamma\tilde{q}_i(t)\\
&+\frac{1}{\varepsilon_1\lambda_{\max}(\hat{L})}\sum_{i=1}^{N}\hat{c}_i\tilde{q}_i^T(t)\Gamma\tilde{q}_i(t)\\
\leq\, & \delta_s^T(t)(I_N\otimes(A^TP+PA)-\underline{c}\lambda_{\min}(\hat{L})\otimes\Gamma)\delta_s(t)\\
&+\frac{(\varepsilon_1-1)(1-\varepsilon_2)}{\lambda_{\max}(\hat{L})}\sum_{i=1}^{N}\hat{c}_i\hat{q}_i^\top(t)\Gamma\hat{q}_i(t)+\frac{\varepsilon_1(\varepsilon_1-1)(1-\frac{1}{\varepsilon_2})+1}{\varepsilon_1\lambda_{\max}(\hat{L})}\sum_{i=1}^{N}\hat{c}_i\tilde{q}_i^T(t)\Gamma\tilde{q}_i(t).
\end{aligned}\tag{3.10}$$

Taking the derivative with respect to $V_3(t)$, we can get

$$\dot{V}_3(t)=\kappa\sum_{i=1}^{N}(\hat{c}_i-\beta)Proj_i(\hat{c}_i,M_i), \tag{3.11}$$

where $\kappa=-\frac{(\varepsilon_1-1)(1-\varepsilon_2)}{\lambda_{\max}(\hat{L})}>0$, and $M_i=\hat{q}_i^T(t)\Gamma\hat{q}_i(t)$.

Combining (3.10) and (3.11), one has

$$\begin{aligned}
e^{\alpha t}\dot{V}_1(t)+\dot{V}_3(t)\leq\, & e^{\alpha t}\delta_s^T(t)(I_N\otimes(A^TP+PA)-\underline{c}\lambda_{\min}(\hat{L})\otimes\Gamma)\delta_s(t)\\
&-e^{\alpha t}\kappa\sum_{i=1}^{N}\hat{c}_i\hat{q}_i^T(t)\Gamma\hat{q}_i(t)+e^{\alpha t}(\frac{\kappa}{\varepsilon_2}+\frac{1}{\varepsilon_1\lambda_{\max}(\hat{L})})\sum_{i=1}^{N}\hat{c}_i\tilde{q}_i^T(t)\Gamma\tilde{q}_i^T(t)\\
&+\kappa\sum_{i=1}^{N}(\hat{c}_i-\beta)Proj_i(\hat{c}_i,M_i)\\
\leq\, & e^{\alpha t}\delta_s^T(t)(I_N\otimes(A^TP+PA)-\underline{c}\lambda_{\min}(\hat{L})\otimes\Gamma)\delta_s(t)\\
&-\kappa\sum_{i=1}^{N}\hat{c}_iM_i+\kappa\beta M_i-\kappa\beta M_i+\kappa\sum_{i=1}^{N}(\hat{c}_i-\beta)Proj_i(\hat{c}_i,M_i)\\
&+e^{\alpha t}\ell\sum_{i=1}^{N}\hat{c}_i\tilde{q}_i^T(t)\Gamma\tilde{q}_i(t)\\
\leq\, & e^{\alpha t}\delta_s^T(t)(I_N\otimes(A^TP+PA)-\underline{c}\lambda_{\min}(\hat{L})\otimes\Gamma)\delta_s(t)\\
&+\kappa\sum_{i=1}^{N}(\hat{c}_i-\beta)(Proj_i(\hat{c}_i,M_i)-M_i)+e^{\alpha t}\ell(\hat{c}_i\tilde{q}_i^T(t)\Gamma\tilde{q}_i(t)-\frac{\kappa\beta}{\ell}\hat{q}_i^T\Gamma\hat{q}_i(t))\\
\leq\, & e^{\alpha t}\delta_s^T(t)(I_N\otimes(A^TP+PA)-\underline{c}\lambda_{\min}(\hat{L})\otimes\Gamma)\delta_s(t)\\
&+\kappa\sum_{i=1}^{N}(\hat{c}_i-\beta)(Proj_i(\hat{c}_i,M_i)-M_i)+e^{\alpha t}\ell\frac{\eta_i}{\theta_i},
\end{aligned}\tag{3.12}$$

where $\ell = \frac{\kappa}{\varepsilon_2} + \frac{1}{\varepsilon_1 \lambda_{\max}(\hat{L})} > 0$.
Taking the derivative with respect to $V_2(t)$, we can get

$$\dot{V}_2(t) \leq -\sum_{i=1}^{N} \rho_i \eta_i(t) - \frac{\xi_i}{\theta_i} \eta_i(t). \tag{3.13}$$

Then, based on (3.12) and (3.13), we can obtain

$$\begin{aligned}
\dot{W}(t) \leq\, & e^{\alpha t} \delta_s^T(t)(I_N \otimes (A^T P + PA) - \underline{c}\lambda_{\min}(\hat{L}) \otimes \Gamma)\delta_s(t) \\
& + \kappa \sum_{i=1}^{N} (\hat{c}_i - \beta)(Proj_i(\hat{c}_i, M_i) - M_i) \\
& + e^{\alpha t}(\ell \frac{\sum_{i=1}^{N} \eta_i(t)}{\theta_i} - \rho_i \sum_{i=1}^{N} \eta_i(t) - \frac{\xi_i}{\theta_i} \sum_{i=1}^{N} \eta_i(t)) \\
\leq\, & e^{\alpha t} \delta_s^T(t)(I_N \otimes (A^T P + PA) - \underline{c}\lambda_{\min}(\hat{L}) \otimes \Gamma)\delta_s(t) \\
& + \kappa \sum_{i=1}^{N} (\hat{c}_i - \beta)(Proj_i(\hat{c}_i, M_i) - M_i) \\
& - e^{\alpha t}(\rho_i + \frac{\xi_i - \ell}{\theta_i}) \sum_{i=1}^{N} \eta_i(t) \\
\leq\, & -e^{\alpha t} \frac{\lambda_{\min} Q}{\lambda_{\max}(P)} \delta^T(t)(I_N \otimes P)\delta(t) \\
& + \kappa \sum_{i=1}^{N} (\hat{c}_i - \beta)(Proj_i(\hat{c}_i, M_i) - M_i) \\
& - e^{\alpha t}(\rho_i + \frac{\xi_i - \ell}{\theta_i}) \sum_{i=1}^{N} \eta_i(t) \\
\leq\, & -\alpha e^{\alpha t}(V_1(t) + V_2(t)) \\
\leq\, & -\alpha e^{\alpha t} U(t),
\end{aligned}$$

where a positive constant $\alpha = \min\{\frac{\lambda_{\min}(Q)}{\lambda_{\max}(P)}, \rho_i + \frac{\xi_i - \ell}{\theta_i}\}$. This implies that:

$$e^{\alpha t} U(t) \leq W(t) \leq W(T_k + \tau_k + \chi_k), \quad t \in [T_k + \tau_k + \chi_k, T_{k+1}).$$

Then, we have

$$U(t) \leq e^{-\alpha(t - T_k - \tau_k - \chi_k)} W(T_k + \tau_k + \chi_k), \quad t \in [T_k + \tau_k + \chi_k, T_{k+1}).$$

Case 2. When the agent is under DoS attacks, for $t \in \Psi_{att}(t_0, t)$, we can obtain that $\dot{\delta}(t) = (I_N \otimes A)\delta(t)$ due to $u_i(t) = 0$. Then,

$$\dot{V}(t) \leq e^{\alpha t} \delta^T(t)(I_N \otimes (A^T P + PA))\delta(t) + e^{\alpha t} \dot{\eta}(t) + \frac{\kappa}{c} \sum_{i=1}^{N} (\hat{c}_i - \beta)\dot{\hat{c}}_i(t)$$

$$\begin{aligned}
&\leq e^{\alpha t}\frac{\lambda_{\max}(A^T P + PA)}{\lambda_{\min}(P)}\delta^T(t)(I_N \otimes P)\delta(t)\\
&\leq \hat{\alpha} e^{\alpha t} V_1(t)\\
&\leq \hat{\alpha} e^{\alpha t} U(t),
\end{aligned}$$

where $\hat{\alpha} = \frac{\lambda_{\max}(A^T P+PA)}{\lambda_{\min}(P)} > 0$. Because of $\dot{W}(t) = \dot{V}(t) + \alpha e^{\alpha t} U(t)$, where $\dot{V}(t) = e^{\alpha t}\dot{U}(t) + \dot{V}_3(t)$, we have

$$\begin{aligned}
\dot{W}(t) &\leq e^{\alpha t}(\alpha + \hat{\alpha})U(t)\\
&\leq (\alpha + \hat{\alpha})W(t). \qquad (3.14)
\end{aligned}$$

According to (3.14), we can obtain

$$W(t) \leq e^{(\alpha+\hat{\alpha})(t-T_k)} W(T_k), \quad t \in [T_k, T_k + +\tau_k + \chi_k).$$

Also, we have $e^{\alpha} U(t) \leq W(t)$, that is,

$$U(t) \leq e^{\hat{\alpha}(t-T_k)} W(T_k), \quad t \in [T_k, T_k + +\tau_k + \chi_k).$$

Thus, according to Case 1 and Case 2, for $t \in [T_k + \tau_k + \chi_k, T_{k+1})$, one gets

$$\begin{aligned}
U(t) &\leq e^{-\alpha(t-T_k-\tau_k-\chi_k)} W(T_k + \tau_k + \chi_k)\\
&\leq e^{-\alpha(t-T_k-\tau_k-\chi_k)} e^{\hat{\alpha}(\tau_k+\chi_k)} W(T_k)\\
&\leq \ldots \leq\\
&\leq e^{-\alpha(t-\Psi^*_{\text{att}}(t_0,t))} e^{\hat{\alpha}(\Psi^*_{\text{att}}(t_0,t))} W(0). \qquad (3.15)
\end{aligned}$$

When $t \in [T_k, T_k + \tau_k + \chi_k)$, we have

$$\begin{aligned}
U(t) &\leq e^{\hat{\alpha}(t-T_k)} W(T_k)\\
&\leq e^{\hat{\alpha}(t-T_k)} e^{-\alpha(T_k-T_{k-1}-\tau_{k-1}-\chi_{k-1})} W(T_{k-1} + \tau_{k-1} + \chi_{k-1})\\
&\leq \ldots \leq\\
&\leq e^{-\alpha(t-\Psi^*_{\text{att}}(t_0,t))} e^{\hat{\alpha}(\Psi^*_{\text{att}}(t_0,t))} W(0). \qquad (3.16)
\end{aligned}$$

Based on (3.15) and (3.16), it can be concluded that

$$U(t) \leq e^{-\alpha(t-\Psi^*_{\text{att}}(t_0,t))} e^{\hat{\alpha}(\Psi^*_{\text{att}}(t_0,t))} W(0). \qquad (3.17)$$

From (3.17), we have

$$\begin{aligned}
U(t) &\leq e^{((\alpha+\hat{\alpha})(\Psi^*_{\text{att}}(t_0,t))-\alpha t)} W(0)\\
&\leq e^{(\alpha+\hat{\alpha})(\Psi(t_0,t)+\wp(t_0,t)\chi)-\alpha t} W(0)\\
&\leq e^{(\alpha+\hat{\alpha})(N_1+N_2\chi)} e^{[(\alpha+\hat{\alpha})(\frac{1}{\Omega_1}+\frac{\chi}{\Omega_2})-\alpha]t} W(0). \qquad (3.18)
\end{aligned}$$

According to (3.18), if the sufficient condition Theorem 3.1 holds, then $[(\alpha + \hat{\alpha})(\frac{1}{\Omega_1} + \frac{\chi}{\Omega_2}) - \alpha] < 0$. Therefore, the Lyapunov function $V(t)$ asymptotically converges to zero as $t \to \infty$. Since $V(t) > 0$, and $\delta_i(t) = x_i(t) - s_i x_0(t)$, it follows that $\delta_i(t) \to 0$ as $t \to \infty$. Consequently, the followers can achieve leader-following bipartite consensus under DoS attacks.

Remark 3.3. *From the proof of Theorem 3.1, the resilience of the MAS against DoS attacks is closely related to the transformed signed topology. Specifically, $\lambda_{\min}(\hat{L})$ and $\lambda_{\max}(\hat{L})$ affect the algebraic Riccati equation (ARE) solution P and the decay rate α. A denser topology or stronger interaction weights can enlarge the eigenvalue margin of $\hat{L}$, thereby strengthening the stabilizing effect of the control protocol. Moreover, from $\frac{1}{\Omega_1} + \frac{\chi}{\Omega_2} \leq \frac{\alpha}{\alpha+\hat{\alpha}}$, a larger α and a smaller $\hat{\alpha}$ imply stronger tolerance to DoS-active intervals, which explains the enhanced robustness and faster recovery of highly connected MASs.*

Theorem 3.2. *Under the conditions about triggering parameters stated in Theorem 3.1, the adaptive DET control is guaranteed to be free of Zeno behavior.*

Proof. To prove by contradiction, we first assume that the Zeno phenomenon does occur. This implies the existence of a finite $T > 0$ satisfying $\lim_{k\to\infty} t_k^i = T$, which implies $\lim_{k\to\infty}(t_{k+1}^i - t_k^i) = 0$.

$$\tilde{q}_i(t) = \sum_{i=0}^{N} |a_{ij}|(\tilde{x}_i(t) - sgn(a_{ij})\tilde{x}_j(t)) + |l_{i0}|(\tilde{x}_i(t) - s_i\tilde{x}_0(t)),$$

where $\tilde{x}_i(t) = x_i(t) - \hat{x}_i(t)$.

$$\begin{aligned}
D^+\|\tilde{q}_i(t)\| &\leq \|\dot{\tilde{q}}_i(t)\| \leq \|\dot{q}_i(t)\| \\
&\leq \|Aq_i(t) + B\sum_{i=1}^{N}|a_{ij}|(u_i(t) - sgn(a_{ij})u_j(t)) + B|l_{i0}|u_i(t)\| \\
&\leq \|A\tilde{q}_i(t) + A\hat{q}_i(t) + B\sum_{i=1}^{N}|a_{ij}|(u_i(t) - sgn(a_{ij})u_j(t)) + B|l_{i0}|u_i(t)\| \\
&\leq \|A\|\|\tilde{q}_i(t)\| + \|A\|\|\hat{q}_i(t)\| + \|B\|\sum_{i=1}^{N}|a_{ij}|\|(u_i(t) - sgn(a_{ij})u_j(t)) + \|B\|\|l_{i0}\|\|u_i(t)\| \\
&\leq \|A\|\|\tilde{q}_i(t)\| + \varpi_i, \qquad (3.19)
\end{aligned}$$

where $\varpi_i = \sup_{t\in[t_k^i,t_{k+1}^i)}\{\|A\|\|\hat{q}_i(t)\| + \|B\|\sum_{i=1}^{N}|a_{ij}|\|(u_i(t) - sgn(a_{ij})u_j(t)) + \|B\|\|l_{i0}\|\|u_i(t)\|\}$. Then, based on (3.19), we have

$$\|\tilde{q}_i(t)\| \leq \frac{\varpi_i}{\|A\|}\left(e^{\|A\|(t-t_k^i)} - 1\right). \qquad (3.20)$$

According to $\dot{\eta}_i(t) > -\rho_i\eta_i(t) - \frac{\xi_i}{\theta_i}\eta_i(t)$, we can obtain

$$\eta_i(t) > \eta_i(0)e^{-\left(\rho_i+\frac{\xi_i}{\theta_i}\right)t}. \qquad (3.21)$$

When $t = t_{k+1}^i$, one gets

$$\theta_i\left(\hat{c}_i(t_{k+1}^i)\tilde{q}_i^\top(t_{k+1}^i)\Gamma\tilde{q}_i(t_{k+1}^i) - \frac{\kappa\beta}{\ell}\hat{q}_i^\top(t_{k+1}^i)\Gamma\hat{q}_i(t_{k+1}^i)\right) = \eta_i(t_{k+1}^i), \qquad (3.22)$$

and

$$\theta_i\bar{c}\lambda_{max}(\Gamma)\|\tilde{q}_i(t_{k+1}^i)\|^2 \geq \eta_i(t_{k+1}^i). \qquad (3.23)$$

Combining (3.20) and (3.23), one has

$$\theta_i \bar{c} \lambda_{max}(\Gamma) \left[\frac{\varpi_i}{\|A\|} \left(e^{\|A\|(t_{k+1}^i - t_k^i)} - 1 \right) \right]^2 \geq \eta_i(0) e^{-\left(\rho_i + \frac{\xi_i}{\theta_i}\right) t_{k+1}^i},$$

that is,

$$t_{k+1}^i - t_k^i \geq \frac{1}{\|A\|} \ln \left[1 + \frac{\|A\|}{\varpi_i} \sqrt{\frac{\eta_i(0) e^{-(\rho_i + \xi_i/\theta_i) t_{k+1}^i}}{\theta_i \bar{c} \lambda_{\max}(\Gamma)}} \right].$$

Since all closed-loop signals are bounded on the finite interval $[0, T)$, there exists a constant $\bar{\varpi}_i > 0$, independent of k, such that $\varpi_i \leq \bar{\varpi}_i$. Let

$$\gamma_i = \rho_i + \frac{\xi_i}{\theta_i}.$$

Since $t_{k+1}^i \leq T$, it follows that

$$t_{k+1}^i - t_k^i \geq \frac{1}{\|A\|} \ln \left[1 + \frac{\|A\|}{\bar{\varpi}_i} \sqrt{\frac{\eta_i(0) e^{-\gamma_i T}}{\theta_i \bar{c} \lambda_{\max}(\Gamma)}} \right] := \tau_i^* > 0.$$

On the other hand, the assumption $\lim_{k \to \infty} t_k^i = T < \infty$ implies

$$\lim_{k \to \infty} \left(t_{k+1}^i - t_k^i \right) = 0.$$

Taking the limit in the preceding lower-bound inequality yields

$$0 \geq \tau_i^* > 0,$$

which is a contradiction. Therefore, the triggering instants cannot accumulate within a finite time, and Zeno behavior is excluded.

4. Numerical simulation

In this section, a MAS consisting of one leader and six followers is considered to validate the proposed scheme. As depicted in Figure 1, the original structurally unbalanced signed graph is processed by Algorithm 1, through which the followers are partitioned into two antagonistic camps and transformed into an equivalent structurally balanced form. This transformation provides the graph-theoretic foundation for the subsequent bipartite consensus analysis. To thoroughly assess the effectiveness and robustness of the proposed adaptive DET control strategy under DoS attacks, the numerical simulation example is designed as follows.

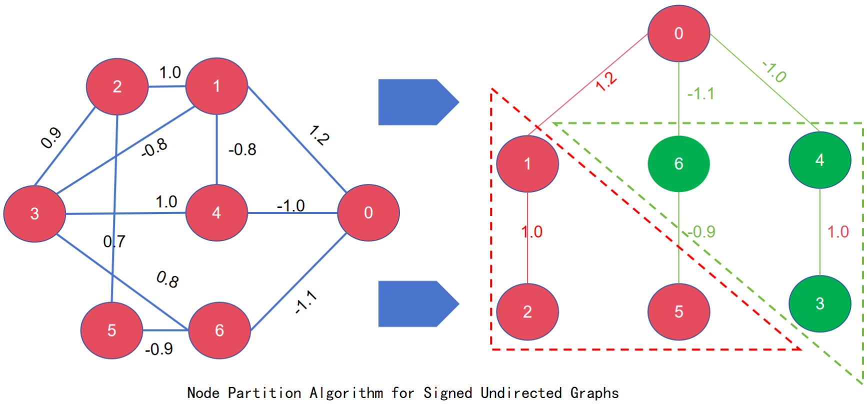

Figure 1. Original and reconstructed communication topologies of the six-agent system.

Example 1. Six agents: In practical networked engineering systems, MASs are often affected by structurally unbalanced interactions, limited communication resources, and malicious DoS attacks, which make it challenging to guarantee accurate cooperative tracking and bipartite consensus. To overcome this challenge, we develop a DET control scheme with projection operator-based adaptive coupling gains. The proposed method reduces unnecessary information transmission, constrains the coupling parameters within a feasible range, and enables follower agents to achieve leader-following bipartite consensus despite intermittent DoS-induced communication interruptions.

According to the ARE, with $Q = I_3$, the matrix P can be obtained as

$$P = \begin{bmatrix} 0.4996 & 0.2483 & 0.1210 \\ 0.2483 & 0.7432 & 0.4213 \\ 0.1210 & 0.4213 & 0.8982 \end{bmatrix}.$$

Then,

$$K = -B^T P = \begin{bmatrix} -0.1210 & -0.4213 & -0.8982 \end{bmatrix}.$$

Moreover,

$$\Gamma = PBB^T P = \begin{bmatrix} 0.0147 & 0.0510 & 0.1087 \\ 0.0510 & 0.1775 & 0.3784 \\ 0.1087 & 0.3784 & 0.8067 \end{bmatrix}.$$

According to Figure 1, one obtains the adjacency matrix $\mathcal{A}$ and the pinning matrix H as follows:

$$\mathcal{A} = \begin{bmatrix} 0 & 1.0 & -0.8 & -0.8 & 0 & 0 \\ 1.0 & 0 & 0.9 & 0 & 0.7 & 0 \\ -0.8 & 0.9 & 0 & 1.0 & 0 & 0.8 \\ -0.8 & 0 & 1.0 & 0 & 0 & 0 \\ 0 & 0.7 & 0 & 0 & 0 & -0.9 \\ 0 & 0 & 0.8 & 0 & -0.9 & 0 \end{bmatrix}, \quad H = \begin{bmatrix} 1.2 & 0 & 0 & 0 & 0 & 0 \\ 0 & 0 & 0 & 0 & 0 & 0 \\ 0 & 0 & 0 & 0 & 0 & 0 \\ 0 & 0 & 0 & -1.0 & 0 & 0 \\ 0 & 0 & 0 & 0 & 0 & 0 \\ 0 & 0 & 0 & 0 & 0 & -1.1 \end{bmatrix}.$$

With all agents initialized randomly, the communication channels of the MAS experience intermittent malicious DoS attacks during the simulation. These attacks are independently applied to different nodes and last for varying time intervals, causing temporary interruptions in the corresponding control inputs. The attacked channels and the time-varying intervals of the associated DoS activities are summarized in Figure 2, which is used to confirm the robustness of the proposed DET bipartite consensus protocol under intermittent communication failures.

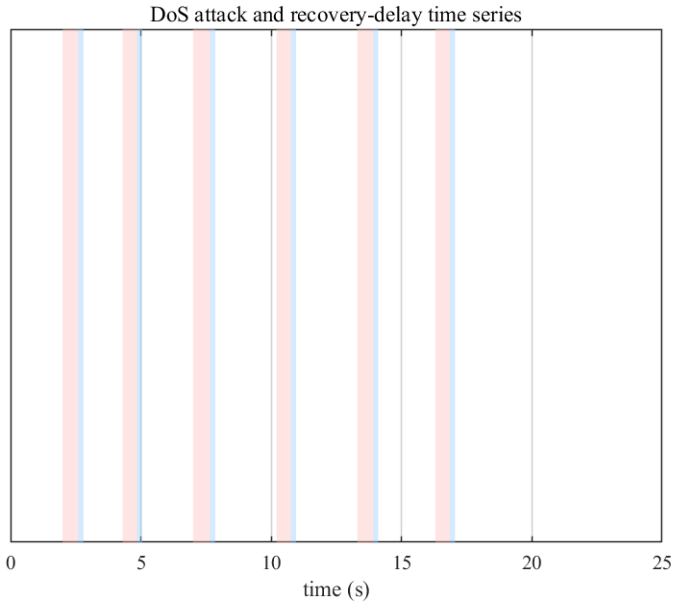

Figure 2. DoS attack intervals.

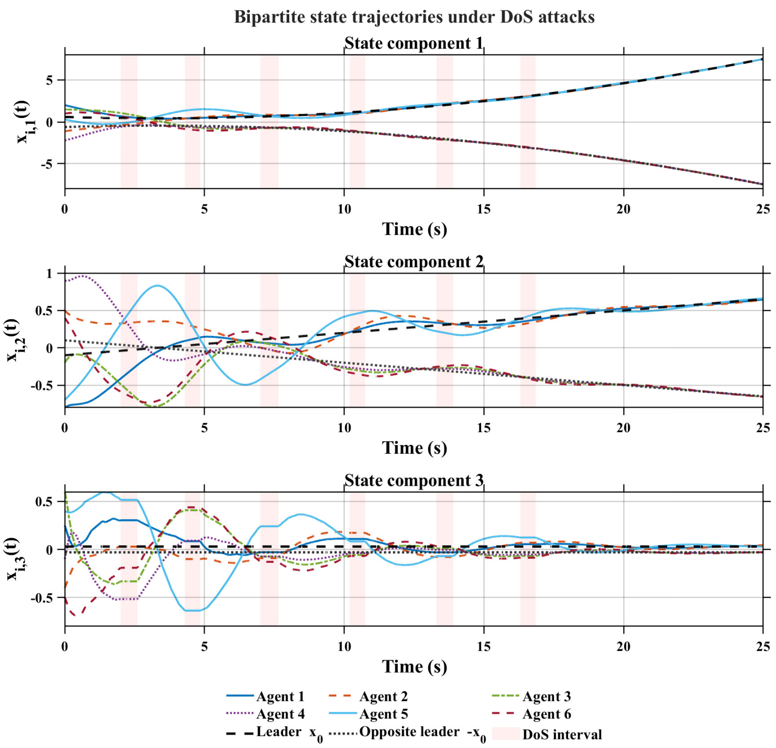

Figure 3. Bipartite state trajectories of the six-agent system under DoS attacks.

To guarantee bipartite consensus under DoS attacks, the DET parameters in the simulation are selected as per Theorem 3.1 conditions. The adaptive coupling gain is constrained by $\underline{c} = 0.15$ and $\bar{c} = 5$, and the event-triggered parameters are chosen as $\varepsilon_1 = \varepsilon_2 = 0.6$, $\theta_i = 0.68$, $\rho_i = 0.36$, $\xi_i = 1.5$, and $b = 1$, $i \in \mathcal{N}$. Solving the ARE yields $\kappa = 0.0578$, $\ell = 0.6989$, $\alpha = 0.7535$, and $\hat{\alpha} = 18.3672$, and thus $\alpha/(\alpha + \hat{\alpha}) = 0.0394$. With $N_1 = 3.5$, $\Omega_1 = 80$, $N_2 = 6$, $\Omega_2 = 20$, and $\chi = 0.2$, we obtain $\frac{1}{\Omega_1} + \frac{\chi}{\Omega_2} = 0.0225 < 0.0394 = \alpha/(\alpha + \hat{\alpha})$, which meets the requirement of Theorem 3.1.

The ultimate goal is to ensure leader-following bipartite consensus in DoS-affected MASs with a signed topology that mixes cooperative and antagonistic interactions. Figure 3 illustrates the multidimensional state trajectories of the leader and all followers over time. It can be observed that the followers in the cooperative camp gradually converge to the leader's trajectory, whereas those in the antagonistic camp converge to the opposite trajectory of the leader, which characterizes bipartite consensus.

The evolution of the bipartite consensus error $x_i - s_i x_0$ for each follower under DoS attacks is shown in Figures 4 and 5. Figure 6 presents the DET instants of each agent under DoS attacks. These results show that, without Zeno behavior, leader-following bipartite consensus tracking remains achievable despite intermittent link attacks.

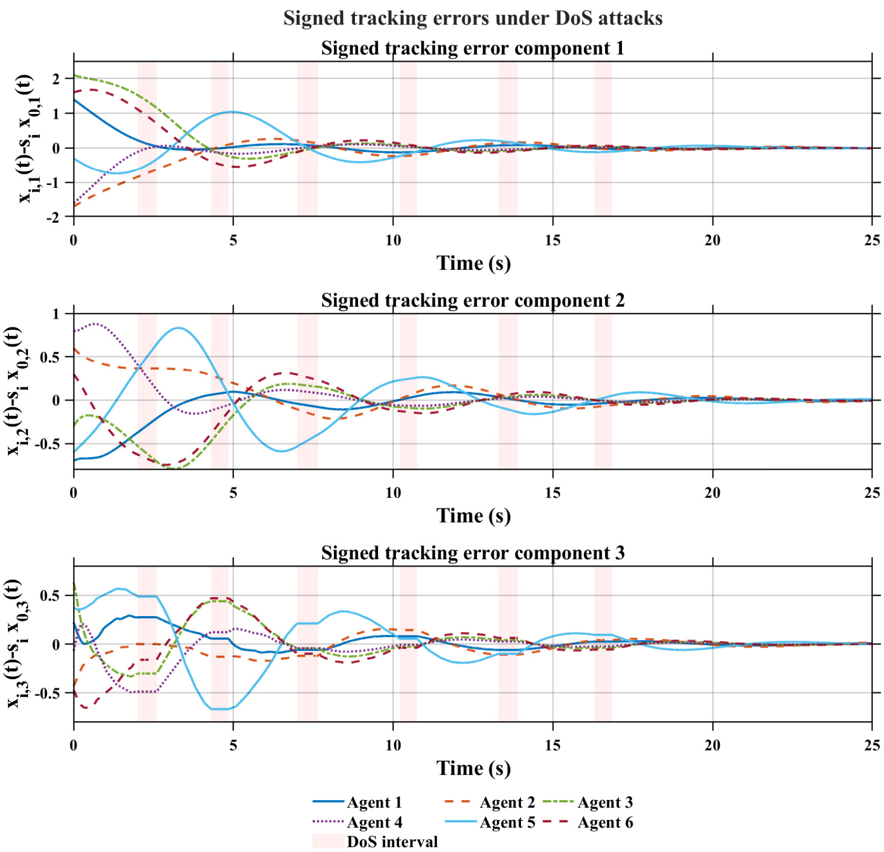

Figure 4. Componentwise bipartite consensus errors of the six-agent system under DoS attacks.

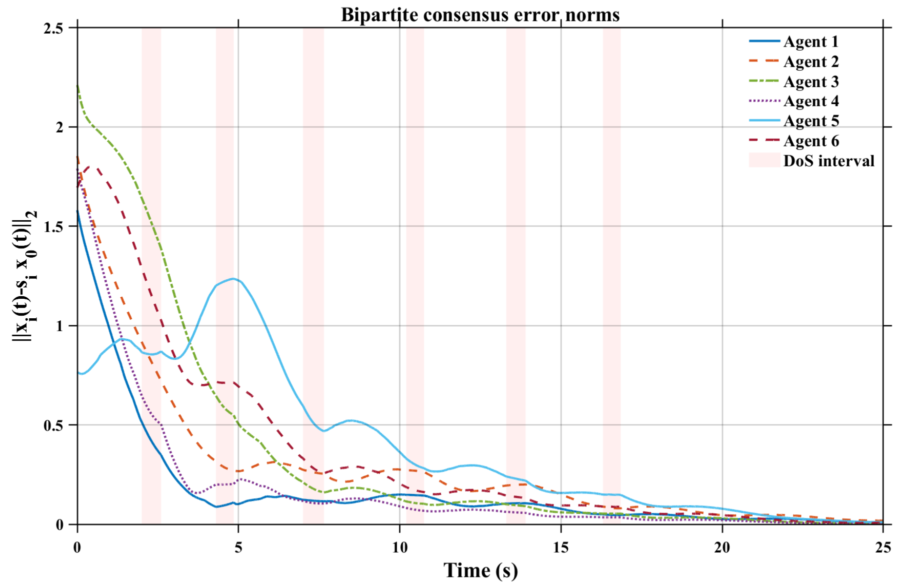

Figure 5. Maximum bipartite consensus error of the six-agent system under DoS attacks.

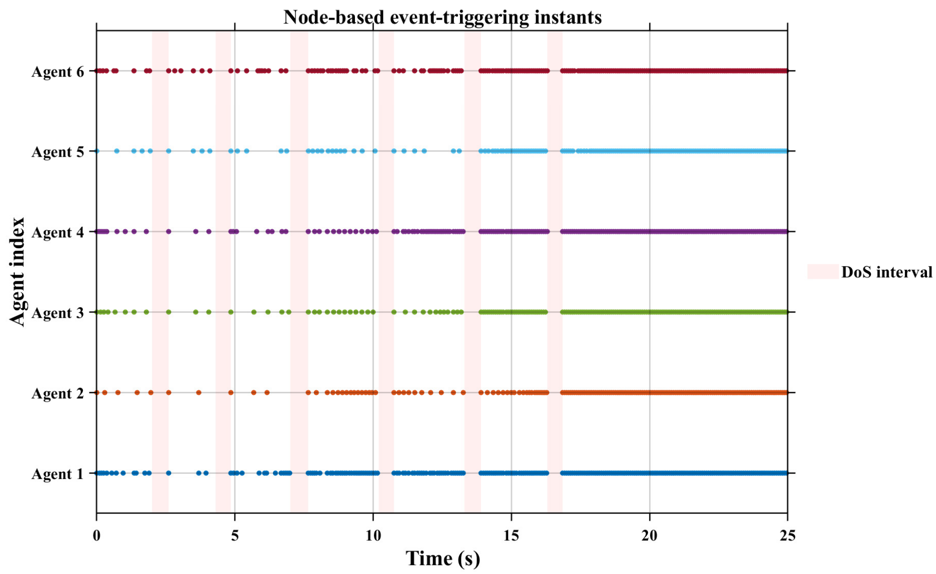

Figure 6. Triggering instants of the six-agent system under DoS attacks.

Figure 7 depicts the evolution of the adaptive coupling parameters in the controller, demonstrating that these parameters can adaptively adjust the control intensity of each node according to the system states, thereby enabling the system to achieve consensus tracking more rapidly.

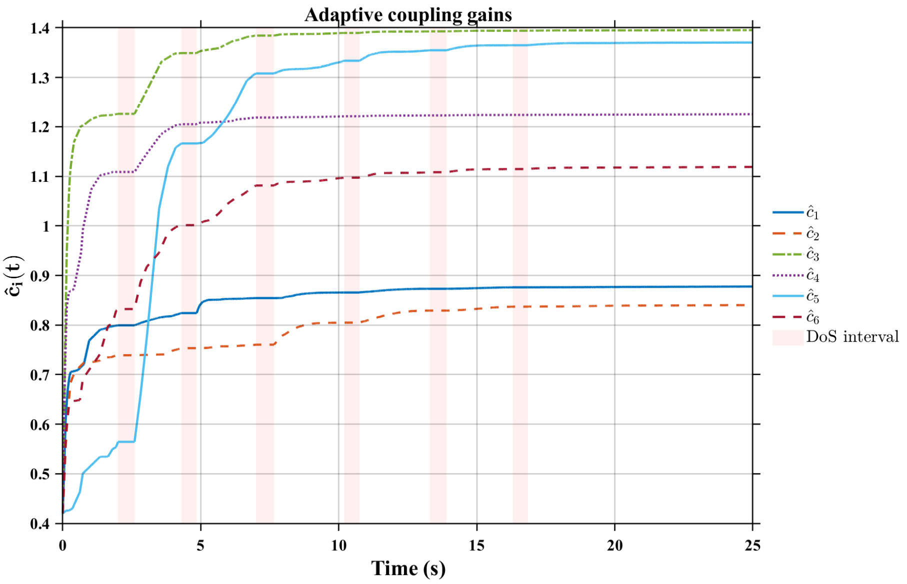

Figure 7. Adaptive coupling gains of the six-agent system under DoS attacks.

Example 2. Ten agents: To further verify the scalability of the proposed method, a ten-agent system with a denser structurally unbalanced topology is considered in Figure 8. As shown in Figure 9, despite repeated DoS attacks, all agents gradually track either the leader trajectory or its opposite, thereby achieving bipartite consensus.

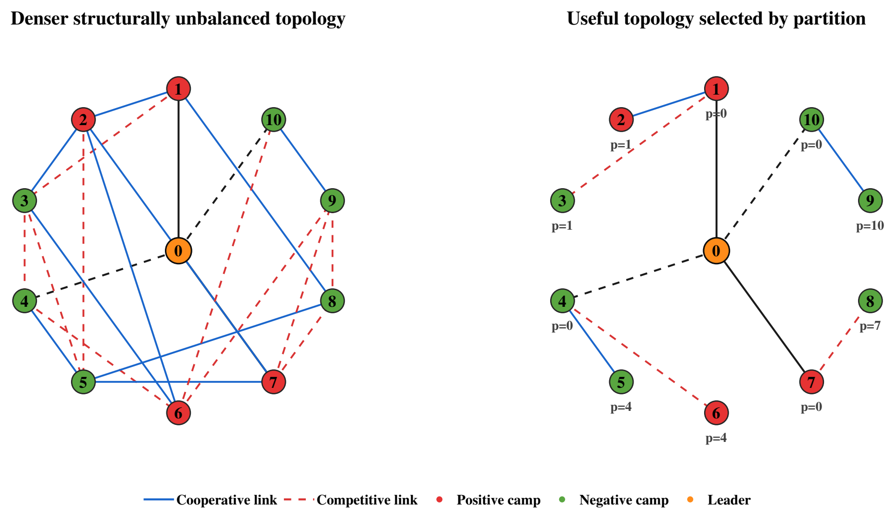

Figure 8. Original structurally unbalanced topology and useful topology selected by the partition algorithm for the ten-agent system.

Figures 10 and 11 show the discrete triggering instants and the evolution of the maximum consensus error, respectively. The error gradually converges to a small neighborhood of zero, while all inter-event intervals remain positive. These results demonstrate the effectiveness and scalability of the proposed method for larger networks under DoS attacks.

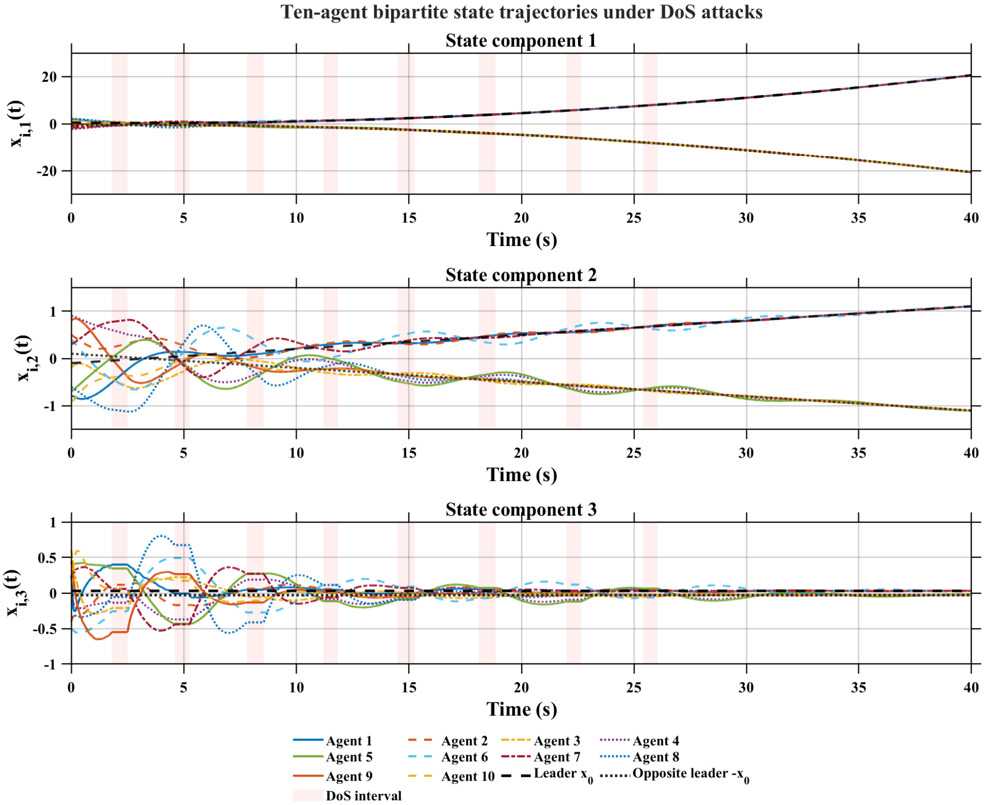

Figure 9. Bipartite state trajectories of the ten-agent system under DoS attacks.

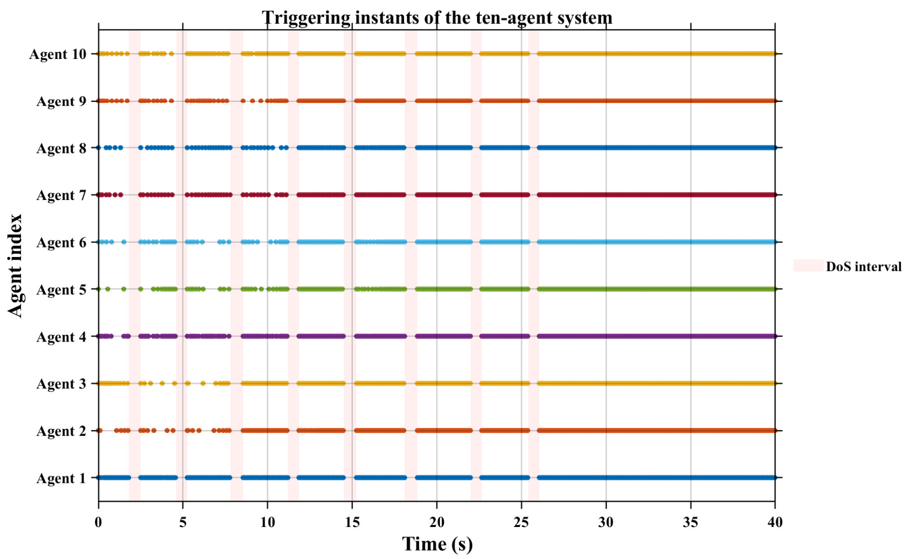

Figure 10. Triggering instants of the ten-agent system under DoS attacks.

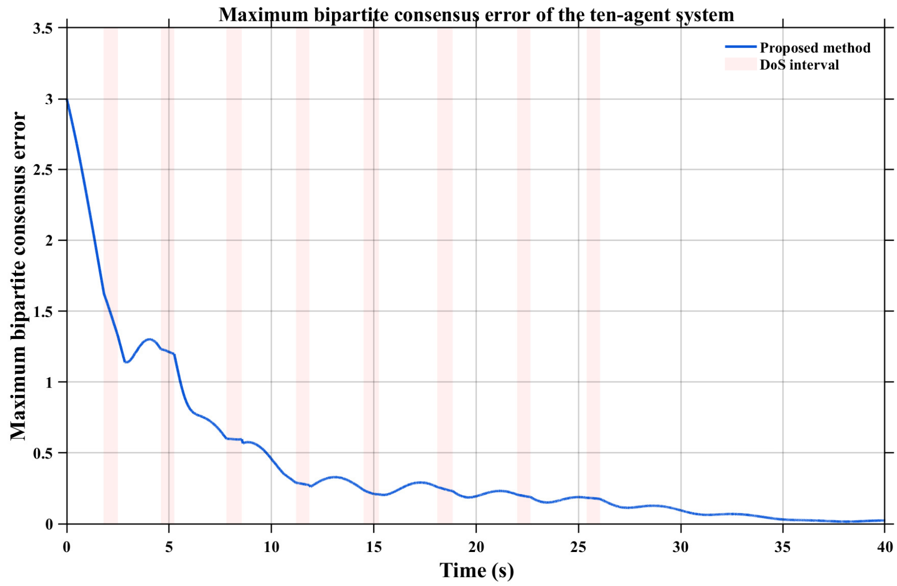

Figure 11. Maximum bipartite consensus error of the ten-agent system under DoS attacks.

Comparative studies. To evaluate the contribution of the projection operator, the proposed method was compared with an unprojected node-based DET baseline adapted from [35] under the same initial conditions, topology, and DoS sequence. As shown in Figure 12 and Table 1, the projection-based method reduces the settling time from 24.334 s to 15.248 s and the final maximum consensus error from 0.038478 to 0.0047707, demonstrating faster and more accurate bipartite consensus under DoS attacks.

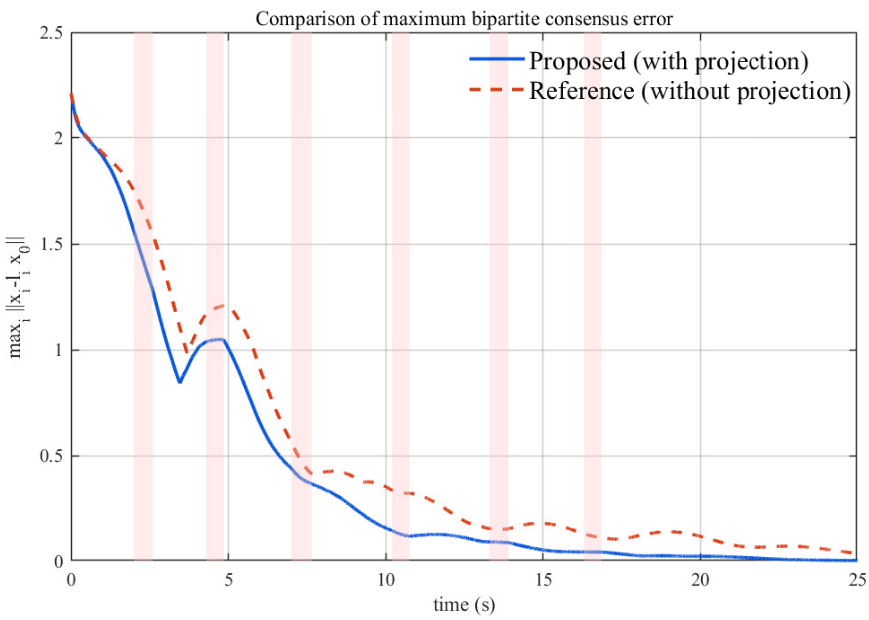

Figure 12. Comparison of maximum bipartite consensus errors under DoS attacks.

Table 1. Performance comparison of the proposed and reference node-based DET strategies under DoS attacks.

	Projection-adaptive node DET	Reference unprojected node DET
Final maximum error	0.0047707	0.038478
Settling time (s)	15.248	24.334

The role of the adaptive coupling gain was further examined using the fixed-gain DET method [36]. As illustrated in Figure 13, the proposed adaptive DET method maintains a lower consensus error during most post-attack intervals and exhibits faster error attenuation. By contrast, the continuous adaptive method of Wu et al. [37] requires real-time information exchange whenever communication is available and therefore provides no communication-saving advantage. These comparisons demonstrate the respective benefits of the projection operator, adaptive gain, and DET mechanism.

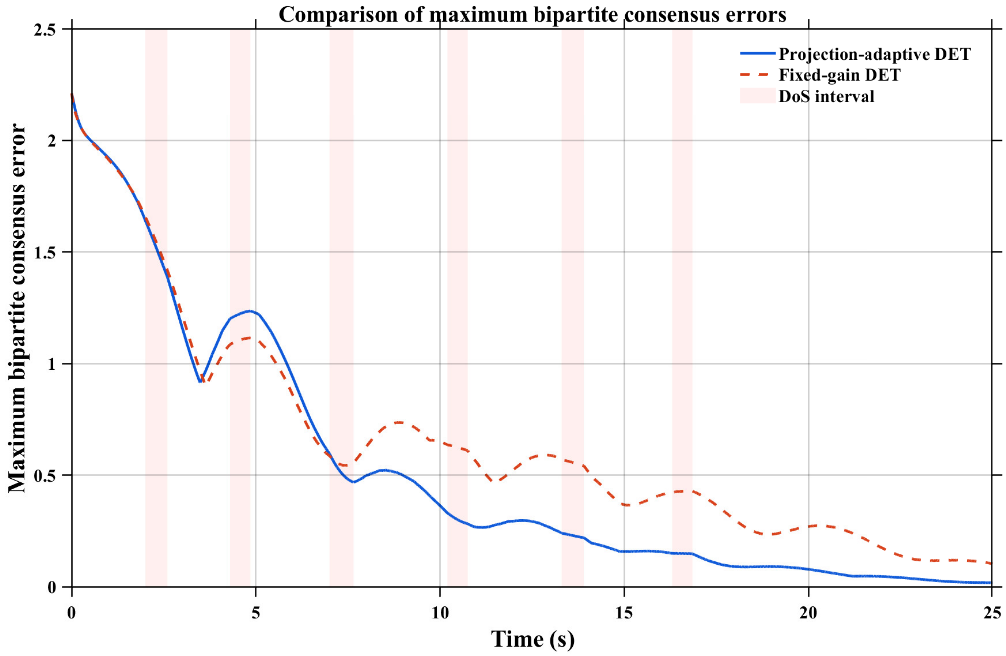

Figure 13. Comparison of the proposed adaptive DET and fixed-gain DET methods under DoS attacks.

5. Conclusions

This paper has presented an adaptive DET control scheme to solve the bipartite consensus problem of MASs under DoS attacks, where the agents are modeled as cooperative and competitive. A projection operator-based adaptive algorithm combined with a DET control scheme has been designed to suppress the infinite growth of adaptive parameters and reduce the communication burden. Besides, a partition algorithm has been proposed to achieve bipartite consensus for the structurally unbalanced topology graph. In addition, rigorous proofs of bipartite consensus and Zeno-behavior exclusion have been provided. In future work, we will extend the DET mechanism to asynchronous DET situations, and the adaptive variables will be doubly coupled.

Author contributions

Xiaoli Ruan: Conceptualization, Methodology, Writing–review and editing; Zhiwei Du: Software, Writing–review and editing, Writing–original draft; Huali Yang: Formal analysis, Project administration, Writing–review and editing; Chen Wang: Formal analysis, Project administration, Writing–review and editing; Jianwen Feng: Supervision, Project administration, Writing–review and editing. All authors have read and approved the final version of the manuscript for publication.

Use of Generative-AI tools declaration

The authors declare that they have not used Artificial Intelligence (AI) tools in the creation of this article.

Acknowledgments

This research was supported by the National Natural Science Foundation of China under grants 62473265, 62301373, 62307029.

Conflict of interest

The authors affirm that they have no conflict of interest.

References

1. R. Olfati-Saber, Flocking for multi-agent dynamic systems: algorithms and theory, *IEEE Trans. Automat. Contr.*, **51** (2006), 401–420. https://doi.org/10.1109/TAC.2005.864190
2. J. Xiao, Y. Li, Deep analysis on MLSY for fractional-order higher-dimension-valued neural networks under the action of free quadratic coefficients, *Expert Syst. Appl.*, **298** (2026), 129586. https://doi.org/10.1016/j.eswa.2025.129586
3. C. Zhao, Y. Chen, K. Shi, L. Zhang, Y. Nie, A relaxed Lyapunov function lemma and genetic algorithm applying to time-delay systems, *Chaos Soliton. Fract.*, **199** (2025), 116687. https://doi.org/10.1016/j.chaos.2025.116687
4. Z. Li, Z. Duan, F. Lewis, Distributed robust consensus control of multi-agent systems with heterogeneous matching uncertainties, *Automatica*, **50** (2014), 883–889. https://doi.org/10.1016/j.automatica.2013.12.008
5. Z. Zuo, R. Ke, Q.-L. Han, Fully distributed adaptive practical fixed-time consensus protocols for multi-agent systems, *Automatica*, **157** (2023), 111248. https://doi.org/10.1016/j.automatica.2023.111248

6. C. Li, D. Zhao, Restoring medical images with combined noise base on the nonlinear inverse scale space method, *Math. Model. Control*, **5** (2025), 216–235. https://doi.org/10.3934/mmc.2025016
7. D. K. Grady, M. Moll, L. E. Kavraki, Extending the applicability of POMDP solutions to robotic tasks, *IEEE Trans. Robot.*, **31** (2015), 948–961. https://doi.org/10.1109/TRO.2015.2441511
8. G. Wen, H. Wang, X. Yu, W. Yu, Bipartite tracking consensus of linear multi-agent systems with a dynamic leader, *IEEE Trans. Circuits Syst. II*, **65** (2018), 1204–1208. https://doi.org/10.1109/TCSII.2017.2777458
9. T. Han, Z.-H. Guan, B. Xiao, H. Yan, Bipartite average tracking for multi-agent systems with disturbances: finite-time and fixed-time convergence, *IEEE Trans. Circuits Syst. I*, **68** (2021), 4393–4402. https://doi.org/10.1109/TCSI.2021.3104933
10. H. Zhao, J. Shan, D. Xu, H. Yu, Dynamic event-triggered bipartite formation for MIMO multiagent systems with quantized data, *IEEE Trans. Cybernetics*, **56** (2026), 619–630. https://doi.org/10.1109/TCYB.2025.3614090
11. J. Cai, J. Yu, Z. You, C. Jing, Event-triggered synchronization for delayed dynamic complex networks via impulsive control strategy, *AIMS Math.*, **11** (2026), 11173–11193. https://doi.org/10.3934/math.2026460
12. B. Zhou, Y. Yang, L. Li, X. Xu, R. Yang, Bipartite consensus for second-order multi-agent systems with external disturbances via constraint data-sampled impulsive method, *Commun. Nonlinear Sci. Numer. Simul.*, **109** (2022), 106314. https://doi.org/10.1016/j.cnsns.2022.106314
13. H. Fan, K. Shi, Z. Guo, A. Zhou, Finite-time synchronization criteria for Caputo fractional-order uncertain memristive neural networks with fuzzy operators and transmission delay under communication feedback, *Fractal Fract.*, **8** (2024), 169. https://doi.org/10.3390/fractalfract8110619
14. C. Xu, H. Xu, H. Su, C. Liu, Adaptive bipartite consensus of competitive linear multi-agent systems with asynchronous intermittent communication, *Int. J. Robust Nonlinear Control*, **32** (2022), 5120–5140. https://doi.org/10.1002/rnc.6086
15. J. Ren, R. Luo, C. Wu, Event-triggered reinforcement learning control for switching fuzzy vehicle lateral dynamics, *IEEE Trans. Intell. Transp. Syst.*, **27** (2026), 5104–5116. https://doi.org/10.1109/TITS.2026.3675136
16. R. Yang, L. Peng, Y. Yang, F. Zhu, Bipartite consensus of linear multi-agent systems by distributed event-triggered control, *J. Syst. Sci. Complex.*, **34** (2021), 955–974. https://doi.org/10.1007/s11424-020-9293-7
17. Y. Cai, H. Zhang, Z. Gao, L. Yang, Q. He, Adaptive bipartite event-triggered time-varying output formation tracking of heterogeneous linear multi-agent systems under signed directed graph, *IEEE Trans. Neural Netw. Learn Syst.*, **34** (2023), 7049–7058. https://doi.org/10.1109/TNNLS.2021.3137393
18. R. Guo, J. Feng, J. Wang, G. Chen, T. Huang, X. Liu, Dynamic event-triggered DMPC with variable prediction horizon for disturbed nonlinear multiagent systems, *IEEE Trans. Control Netw. Syst.*, **12** (2025), 3073–3085. https://doi.org/10.1109/TCNS.2025.3609433

19. R. Guo, J. Feng, X. Wu, J. Wang, T. Huang, H. Zhu, Dynamic self-triggered robust distributed model predictive control for coupled nonlinear systems, *IEEE Trans. Circuits Syst. I*, **72** (2025), 5080–5091. https://doi.org/10.1109/TCSI.2024.3523410

20. C. Yan, L. Yan, Y. Lv, Y. Xia, Dynamic event-triggered Byzantine resilient output regulation in continuous-time high-order multiagent systems with static/dynamic leader, *IEEE Trans. Circuits Syst. I*, **71** (2024), 5532–5545. https://doi.org/10.1109/TCSI.2024.3381191

21. Z. Tang, H. Bian, J. Feng, J. H. Park, Distributed pinning impulsive control on complex networks under dual-channel attacks: An average delayed impulsive gain scheme, *IEEE Trans. Autom. Sci. Eng.*, **22** (2025), 23527–23537. https://doi.org/10.1109/TASE.2025.3627906

22. Y. Sheng, K. Liu, Q. Xiao, T. Huang, G. Zeng, Global exponential stabilization of delayed T–S fuzzy systems on time scales under DoS attacks, *IEEE Trans. Fuzzy Syst.*, **32** (2024), 3237–3246. https://doi.org/10.1109/TFUZZ.2024.3357058

23. X. Ruan, Z. Du, Z. Tang, J. Feng, J. Wang, Bipartite consensus for multi-agent systems under distributed sequential scaling attacks: an edge-based event-triggered scheme, *Appl. Math. Comput.*, **523** (2026), 130025. https://doi.org/10.1016/j.amc.2026.130025

24. Z. Liu, H. Zhang, Z. Wang, Bipartite containment control of multi-agent systems under DoS attacks: an event-triggered scheme, *Int. J. Robust Nonlinear Control*, **35** (2025), 479–495. https://doi.org/10.1002/rnc.7660

25. Q. Wang, L. Zino, D. Tan, J. Xu, W. Zhong, Fully distributed quantized secure bipartite consensus control of nonlinear multiagent systems subject to denial-of-service attacks, *Neurocomputing*, **505** (2022), 101–115. https://doi.org/10.1016/j.neucom.2022.07.047

26. Y. Zhao, H. Sun, J. Yang, L. Hou, D. Yang, Event-triggered fully distributed bipartite containment control for multi-agent systems under DoS attacks and external disturbances, *IEEE Trans. Circuits Syst. I*, **72** (2025), 6011–6024. https://doi.org/10.1109/TCSI.2025.3534241

27. B. Niu, Z. Shang, G. Zhang, W. Chen, H. Wang, X. Zhao, et al., Adaptive fuzzy resilient fixed-time bipartite consensus tracking control for nonlinear MASs under sensor deception attacks, *IEEE Trans. Autom. Sci. Eng.*, **22** (2025), 2542–2551. https://doi.org/10.1109/TASE.2024.3381568

28. B. Niu, Y. Zhu, Y. Liu, Z. Shang, D. Wang, H. Wang, et al., Adaptive fuzzy nonsingular fixed-time bipartite consensus tracking using adding power integration technique for stochastic nonlinear constrained MASs, *IEEE Trans. Fuzzy Syst.*, **33** (2025), 947–958. https://doi.org/10.1109/TFUZZ.2024.3499961

29. Y. Cai, H. Zhang, Z. Gao, L. Yang, Q. He, Adaptive bipartite event-triggered time-varying output formation tracking of heterogeneous linear multi-agent systems under signed directed graph, *IEEE Trans. Neural Netw. Learn. Syst.*, **34** (2023), 7049–7058. https://doi.org/10.1109/TNNLS.2021.3137393

30. M. Zhao, J. Xi, L. Wang, H. Liu, Y. Zheng, Adaptive secure consensus for nonlinear multiagent systems with distributed sequential link attacks under general directed graphs, *Int. J. Robust Nonlinear Control*, in press. https://doi.org/10.1002/rnc.7690

31. T. Swaraj, K. Nath, M. K. Bera, R. K. Mishra, S. Chakraborty, H. R. Karimi, Distributed adaptive barrier function-based integral sliding mode consensus control of multi-agent systems, *ISA Trans.*, **167** (2025), 1330–1338. https://doi.org/10.1016/j.isatra.2025.10.042

32. Z. Li, X. Liu, W. Ren, L. Xie, Distributed tracking control for linear multiagent systems with a leader of bounded unknown input, *IEEE Trans. Autom. Control*, **58** (2013), 518–523. https://doi.org/10.1109/TAC.2012.2208295
33. X. Ruan, Z. Tang, A. Wu, J. Feng, Two-time-scale multi-agent systems under rotation-scale attacks: asynchronous dynamic event-triggered consensus, *Expert Syst. Appl.*, **306** (2026), 130933. https://doi.org/10.1016/j.eswa.2025.130933
34. C. De Persis, P. Tesi, Input-to-state stabilizing control under denial-of-service, *IEEE Trans. Autom. Control*, **60** (2015), 2930–2944. https://doi.org/10.1109/TAC.2015.2416924
35. S. Li, K. Liang, W. He, Fully distributed event-triggered secure consensus of general linear multi-agent systems under sequential scaling attacks, *ISA Trans.*, **127** (2022), 146–155. https://doi.org/10.1016/j.isatra.2022.04.018
36. S. Hu, X. Chen, J. Qiu, F. Zhao, X. Jiang, Y. Du, Dynamic event-triggered bipartite consensus of multiagent systems with estimator and cooperative-competitive interactions, *IEEE Trans. Circuits Syst. II*, **69** (2022), 3309–3313. https://doi.org/10.1109/TCSII.2022.3164782
37. Y. Wu, Q. Liang, Y. Zhao, J. Hu, L. Xiang, Adaptive bipartite consensus control of general linear multi-agent systems using noisy measurements, *Eur. J. Control*, **59** (2021), 123–128. https://doi.org/10.1016/j.ejcon.2021.03.002